Available online at www.sciencedirect.com
SCIENCE DIRECT
Journal of Chromatography B, 834 (2006) 42–47
JOURNAL OF CHROMATOGRAPHY B
www.elsevier.com/locate/chromb

The mechanism of action of α-amylase from *Lactobacillus fermentum* on maltooligosaccharides

Pascale Talamond *, Michel Noirot, Alexandre de Kochko

Institut de Recherche pour le Développement, UMR 141, 911 av. d'Agropolis, BP 64501, 34394 Montpellier, Cedex 5, France

Received 30 September 2005; accepted 5 February 2006
Available online 13 March 2006

Abstract

The action pattern of *Lactobacillus fermentum* α-amylase (FERMENTA) was examined using a series of maltooligosaccharides (G2–G7) as substrates. Structurally, this enzyme has a molecular mass (106 kDa) almost twofold higher than α-amylases from mammalians and cereals. The product pattern was investigated through an analysis of products and substrates using HPAEC with pulsed amperometric detection. FERMENTA was consistent with an endo-type of amylase. The bond cleavage frequencies were studied using maltooligosaccharides of various chain lengths as substrate, i.e. maltose up to maltoheptaose and DP 4900-amylose catalyzed by FERMENTA. The catalytic efficiency (k_{cat}/K_m) increased with chain length from maltose (8.7×10^4 M^{-1} s^{-1}) up to amylose (1×10^9 M^{-1} s^{-1}). These action pattern results revealed that FERMENTA can readily cleave the third linkage from the reducing end of the maltooligosaccharides (G5–G7).

Keywords: Alpha-amylase; Maltooligosaccharide hydrolysis kinetics; *Lactobacillus fermentum*; Maltooligosaccharides; Catalytic efficiency

1. Introduction

In many Africa countries, starchy fermented products are key staple foods and fermentation is one of the oldest and most cost-effective methods of producing and preserving food [1]. In Benin, for instance, ogi, a traditional maize-based fermented weaning food, accounts for more than half of the local diet.

Starch fermentation using an amylolytic *Lactobacillus* strain improves digestibility and could thus be beneficial, especially for young children who are often hampered by inadequate secretion of pancreatic α-amylase (EC 3.2.1.1) [2]. Among various *Lactobacillus* strains that exhibit amylolytic activity, two were isolated: *Lactobacillus fermentum* ogi E1 and *L. fermentum* mawè Mw2 [3]. A new α-amylase from *L. fermentum* ogi E1 (FERMENTA) was isolated and compared with other *Lactobacillus* α-amylases [4].

Some characteristics of FERMENTA have already been described. It has a molecular mass (106 kDa) about twofold higher than α-amylases from mammalians and cereals [5,6], whereas its p*I* (3.6) is lower than that of those other α-amylases (>4.5). The FERMENTA amino acid sequence contains two equal parts: N-terminal moiety with the active site and C-terminal repeated sequences. Using a fold recognition approach, we can predict the structure and function of these repeated sequences. Using two different prediction programs, the C-terminal domain is appear to be organized in β–sheet structures and may constitue the starch binding domain. Moreover, the results of FERMENTA inhibition kinetics indicated that this amylase contains, in addition to the active site, a second soluble carbohydrate binding site needed for its activity [4], similarly to the porcine pancreatic α-amylase (PPA) [7] and the barley α-amylase (AMY) [8]. On the other hand, the action pattern of FERMENTA has not yet been examined on short substrates, nor has the way α-amylase attacks its substrate been described from the standpoint of the location of attack on the substrate and the product formed.

One characteristic of α-amylase is that it catalyses the hydrolysis of internal α-1,4-glucosidic bonds in starch and related saccharides [9]. Two types of soluble substrates are used: long substrates (e.g. amylase) and short substrates (e.g.

Abbreviations: HPAEC, high performance anionic exchange chromatography; PAD, pulsed amperometric detection; FERMENTA, *Lactobacillus fermentum* α-amylase; PPA, porcine pancreatic α-amylase; AMY, barley α-amylase; G_1, glucose; G_2, maltose; G_3, maltotriose; G_4, maltotetraose; G_5, maltopentaose; G_6, maltohexaose; G_7, maltoheptaose; DP, degree of polymerization

* Corresponding author. Tel.: +33 467 41 62 51; fax: +33 467 41 62 22.
E-mail address: talamond@mpl.ird.fr (P. Talamond).

1570-0232/$ – see front matter © 2006 Elsevier B.V. All rights reserved.
doi:10.1016/j.jchromb.2006.02.005

maltodextrines or maltooligosaccharides). Several methods are available to elucidate the action pattern of these enzymes differing by the substrates used: limit dextrins [10], modified starch [11], maltooligosaccharides [12] and maltooligosaccharide derivatives (containing 4-nitrophenyl, or reducing end labeled, etc.) [13]. A method using maltooligosaccharide series from maltose and maltoheptaose was used to study the hydrolysis of animal α-amylase (PPA) and cereal α-amylase AMY [14–16].

Kinetic studies on amylase and the analysis of products of the reaction showed that the active site is organized in subsites, each of them accommodating a glucose residues. Each subsite is numbered according to the position of the reducing end of the sugar, i.e. 1, 2, 3, ... and −1, −2, −3, ..., respectively to the reducing end and nonreducing end. The cleavage site is located between the subsites 1 and −1. The structural organization with five subsites was proposed for bacterial (*Bacillus subtilis*) and mammalian amylases (Fig. 1). The active site is directed to receive polymers of the nonreducing end at the reducing end. The catalytic site (arrow in Fig. 1) is the cleavage site. α-amylases contain 5–10 subsites, each receiving a monomer of the substrate via hydrogen bonds and hydrophobic interactions [17–21]. The number of subsites and the binding energy at each subsite may be deduced by experimentally determining the kinetic parameters, i.e. Michaelis constant (K_m), catalytic activity (k_{cat}) and catalytic efficiency (k_{cat}/K_m), and the cleavage frequency at the bonds of the polymeric substrate [15]. The 3D structure of different α-amylase/inhibitor complexes made it possible to accurately describe the active site of amylases, particularly that of the APP [22].

The present study was aimed at determining the action pattern of α-amylase from *L. fermentum* (FERMENTA). We carried out a large number of kinetic experiments with maltooligosaccharide series and amylose. The digestion products were analyzed by HPAEC to determine the bond cleavage frequencies and catalytic efficiencies by FERMENTA for maltoligosaccharides containing two to seven glucose residues. These maltooligosaccharides can be used for studies on the action pattern of FERMENTA.

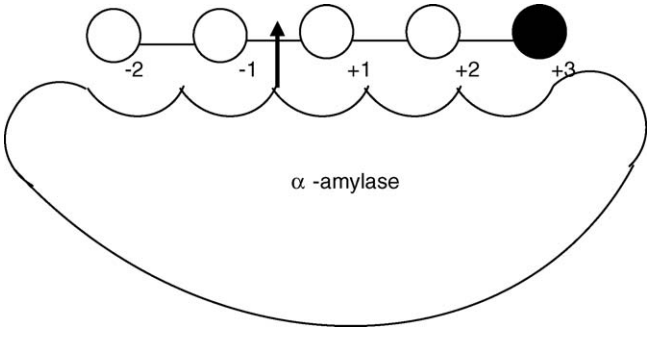

Fig. 1. Structural organization of subsites of α-amylase active sites: (◡) enzyme subsite; (◯) glucose unit; (↓) cut position; and (●) reduced glucose unit.

2. Materials and methods

2.1. Materials

2.1.1. Reagents

A Waters MonoQ (Milford, MA, USA) column (ProteinPak™ Q 15HR, 10 mm × 100 mm), polymeric strong anion exchange with 15 μm size particule was used. Soluble starch, amylose (type III from potato) DP 4900 (794 kDa) [23], β–cyclodextrin, maltose, maltooligosaccharides, triethanolamine, phenylmethylsulfonylfluoride (PMSF), diisopropylfluorophosphate (DFP) and the protease inhibitor cocktail were from Sigma (St. Louis, MO, USA). All other chemicals used in this study were analytical grade. The Ceralpha kit (Megazyme, Ireland) was used to determine α-amylase activity during purification.

2.1.2. Instrumentation

LC analyses were performed with high-performance anion-exchange chromatography (HPAEC) (Dionex, Sunnyvale, CA, USA) equipped with a gradient pump (GP 40), a pulsed amperometric detector (ED 40) and an autosampler TSP AS3500 (Spectra System, USA) was used to inject samples. The Dionex Peaknet 5.1. software package was used for data collection and processing.

2.1.3. Sample preparation

Lactobacillus fermentum Ogi E1 (I-2028, CNCM, Institut Pasteur, Paris) was cultured according to Agati et al. [3]. FERMENTA was purified as previously described by Talamond et al. [4]. The amylase concentrations were determined by measuring A_{280} nm ($\varepsilon^{1\%} = 24$) by using molar absorption coefficient $13.8 \times 10^4\ M^{-1}\ cm^{-1}$ as amylase reference (PPA).

2.2. Methods

2.2.1. Chromatographic conditions

Separation was carried out with a CarboPac PA-100 (4 mm × 250 mm, 5 μm) column equipped with a guard-column (CarboPac PA). The elution was performed with a 5–500 mM sodium acetate gradient over 20 min in 100 mM NaOH at room temperature and at 1.0 ml min^{-1}. A 20-μL constant volume injection loop was used throughout. Detection was performed by triple-pulsed amperometry using an amperometric detector (ED 40) with a gold working electrode. At the exit of the column, the secondary function alcohol of the oligosaccharides at high pH, was oxidized at the surface of a gold electrode by the application of detection potentials. The current generated is proportional to the carbohydrate concentration, thus providing a mean for the quantitative detection. The advantage of this method is its high sensitivity (order of the picomole). The pulse potential and duration used are showed in Table 1. For quantification, glucose, maltose, maltotriose, maltotetraose, maltopentaose, maltohexaose, and maltoheptaose (0.5–5 μM) were used as calibration standards. The quantity of each of them was determined by the measurement of the peak surface of about

Table 1
Amperometric detector (ED 40) timed events

Time (s)	Potential (V)
0.00	0.10
0.20	0.10
0.40	0.10
0.41	−2.0
0.42	−2.0
0.43	0.6
0.44	−0.10
0.40	−0.10

10–20 nC. The concentration zone between 0.5 and 7 μM is linear for each maltooligosaccharides.

2.2.2. Kinetic experiments

Kinetic experiments were performed at 40 °C in 20 mM sodium acetate buffer (pH 5.0), containing 1 mM $CaCl_2$ and 1 mM sodium azide. Substrate and buffer were mixed and the reaction was initiated by adding the enzyme.

When maltoolgosaccharides were used as substrate, the incubation volume was 225 μL with an enzyme volume of 25 μL. Samples (40 μL) were removed at the appropriate time intervals (0, 0.15, 0.30, 0.45, and 1 min), added to 500 mM sodium carbonate to stop the reaction of each oligosaccharide and kept on ice until analysis. Aliquots were then injected in the Dionex system. The above-described conditions enabled us to determine the initial velocity of the hydrolysis time course. The kinetic parameters were determined at the lowest possible substrate concentrations in order to limit transglycosylation and condensation. The hydrolysis rate was determined by measuring the maltooligosaccharides produced.

When amylose was the substrate, amylase activity was determined by reductometry [24]. The incubation volume was 400 μL with an enzyme volume of 100 μL. The reaction was stopped at the appropriate time intervals (1, 3, and 5 min) by adding 500 μL of chilled 0.38 M sodium carbonate containing 1.8 M cupric sulfate and 0.2 M glycine (500 μL) and kept on ice. The hydrolysis rate of DP 4900-amylose was determined on the basis of the increase in reducing power when using maltose as standard. The reductometry or HPAEC-PAD values gave initial velocities as calculated from the slopes obtained by linear regression of the linear part of the progress curves, which in turn gave the number of glycoside bonds hydrolysed per minute or the amount of product (G1, G2, G3, G4, G5, and G6) released per minute, respectively. All experiments were conducted in triplicate or quadruplicate (with experimental error <5%).

2.2.3. Theoretical method

The rate of decrease in substrate can be assumed to obey first-order kinetics, and the reaction was performed at much lower substrate concentrations than K_m, according to the Michaelis–Menten equation:

$$v = -\frac{d(S)}{dt} = \frac{k_{cat}}{K_m}[E_0][S]$$

or

$$\ln\frac{[S_0]}{[S]} = \frac{k_{cat}}{K_m}[E_0]t$$

where $[E_0]$ and $[S_0]$ are the added concentrations of enzyme and substrate, and $[S]$ is the concentration of substrate at any time during hydrolysis.

The catalytic efficiency k_{cat}/K_m was determined from the $\ln[S_0]/[S]$ versus t plot. The k_{cat}/K_m catalytic efficiency slope values were calculated by linear regression.

3. Results

3.1. Hydrolysis of maltoheptaose (G7) and maltohexaose (G6) by α-amylase

Maltoheptaose and maltohexaose were used at various concentrations in the FERMENTA reaction to determine the product pattern tested by high-performance anion-exchange chromatography (Fig. 2). All oligosaccharides were detected with a pulsed amperometric detector. The initial velocities of the hydrolysis reactions with these two substrates were measured for different substrate concentrations. Assessment of the distribution patterns of the products at various concentrations indicated that these distributions varied according to the initial substrate concentration (Fig. 3). For maltoheptaose and maltohexaose, the hydrolysis product profiles changed according to the initial substrate concentration substrate and oppose the concentration of 500 μM to both others. However, the patterns obtained at 500 μM concentration were different.

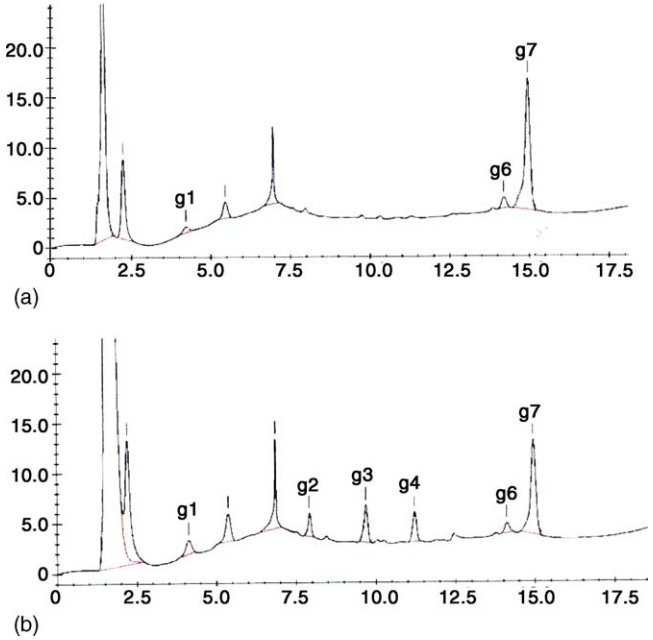

Fig. 2. Separation of maltooligosaccharides in the DP 1-7 range: (a) at time zero; (b) at 30 min of maltoheptaose (100 μM) hydrolysis by FERMENTA (1 μM).

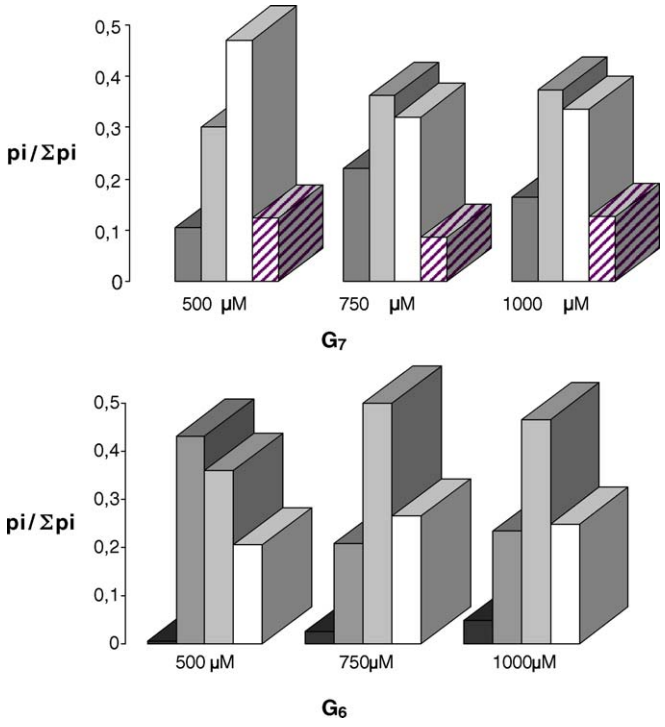

Fig. 3. Product distribution patterns for maltoheptaose and maltohexaose at various substrate concentrations. Substrate concentrations are given on the abscissa axis. Product: (■) glucose; (■) maltose; (■) maltotriose; (□) maltotetraose; and (▨) maltohexaose.

3.2. Amylose hydrolysis by FERMENTA

This study involved determining the kinetic parameters of hydrolysis catalysed by FERMENTA and a substrate with long chain polysaccharides, i.e.: amylase (Fig. 4). The hydrolysis reaction was initiated by the addition of amylase (2 nM) in the reaction medium (buffer and substrate) by reductometry [24]. Seven amylose concentrations ranging from 0.05 to 1.26 μM (or 0.04 to 1 g L^{-1}) were used, with each experiment carried out in quadruplicate. The initial velocity is given in the linear part of the kinetics $[S]=f(t)$, near to the origin. The results are expressed using a Michaelis–Menten $v = f([S])$ plot and Lineweaver–Burk $1/v = f(1/[S])$ plot. The kinetic study generated plots in double reverse $1/v_i = f(1/[S])$ linear. Relationships between the initial velocity and the substrate concentration were hyperbolic. The slope of the $1/v$ line corresponded to the catalytic efficiency. From the experimental values, a statistical analysis allowed us to compute k_{cat} and K_m and then the catalytic efficiency k_{cat}/K_m (1×10^9 M^{-1} s^{-1}) for FERMENTA.

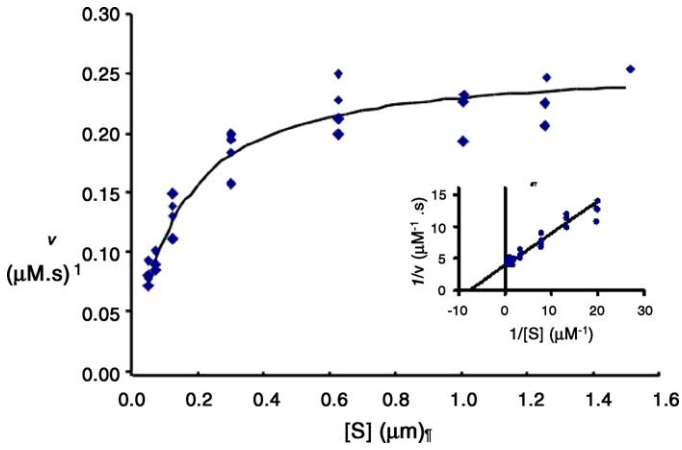

Fig. 4. Amylose hydrolysis by FERMENTA (2 mM). Michaelis–Menton plot $v = f([S])$. (Insert) Lineweaver–Burk plot $1/v = f(1/[S])$.

3.3. Catalytic efficiencies

From the optimum conditions (pH 5.0) and 40 °C temperature in sodium acetate buffer, the kinetic parameters were determined using six oligosaccharides (G2–G7) as substrate with a fixed concentration (10 μM). After incubation, the reactions were initiated by the addition of enzyme (1–100 nM). Samples collected every 15 s to 1 min were analyzed by HPAEC giving [*S*], i.e. the amount of substrate remaining at each time (Fig. 4). The initial substrate $[S_0]$ and enzyme $[E_0]$ concentrations are given in Table 2. The relationships between $(\ln [S_0]/[S])$ and time were linear for all maltooligosaccharides from G2 to G7 (see insert Fig. 4). The slope values gave the k_{cat}/K_m directly (Table 2). Catalytic efficiencies increased with the length of the substrate, from maltose to maltoheptaose. This increase reached almost 200-fold from G2 to G7. The catalytic efficiencies markedly increased between Glc3 and Glc4 (74-fold) and remained almost stable between G4 and G7.

3.4. Cleavage frequencies

When the substrate concentrations were less than 0.1 K_m, the released products were quantified using the corresponding standard at various incubation times. Under these conditions (with low substrate concentrations), a linear relation was obtained for each substrate (G3–G7) with respect to the product concentration over time (insert Fig. 5). For each hydrolized product, the initial velocity (v_i) was calculated by the slope straight line $p=f(t)$. The cleavage frequency ($v_i/\Sigma v_i$) indicated the binding mode of the corresponding substrate. For a given substrate

Table 2
Catalytic efficiency in the hydrolysis of different substrates, i.e. G_2–G_7 (100 μM), by FERMENTA determined at the indicated enzyme concentrations

	Substrate					
	Glc2	Glc3	Glc4	Glc5	Glc6	Glc7
k_{cat}/K_m (s^{-1} M^{-1})	8.7×10^4	9.3×10^4	6.9×10^6	1.6×10^7	1.6×10^7	1.9×10^7
E_0 (μM)	100	100	1	1	1	1

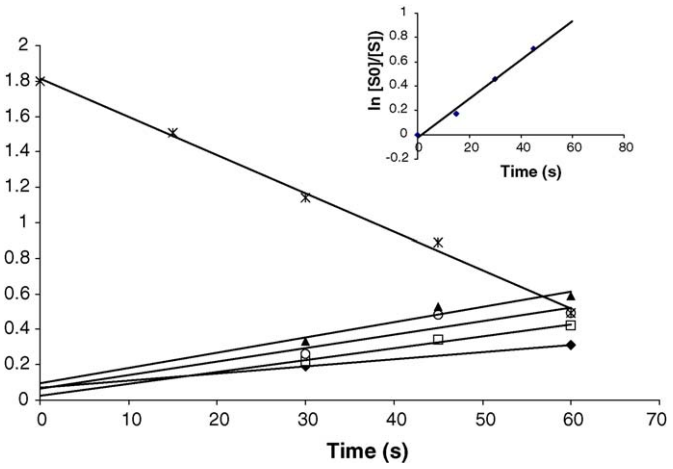

Fig. 5. Maltoheptaose hydrolysis catalyzed by FERMENTA. (insert) $\ln(\{S_0\}/\{S) = f(t)$ plot: (✱) maltoheptaose; (◯) maltotetraose; (▲) maltotriose; (□) maltose; and (♦) glucose.

Table 3
Cleavage frequency for maltooligosaccharide (G4, G5, G6, and G7) hydrolysis

Substrate	Reaction products (%)			
	G1	G2	G3	G4
Maltoheptaose	0.12	0.255	0.34	0.283
Maltohexaose		0.41	0.424	0.166
Maltopentaose	0.18	0.494	0.376	
Maltotetraose	0.49	0.371	0.136	

(G4–G7), reproducible values were obtained at four incubation times. Each hydrolysis proceeded until no more than 10% of the substrate was hydrolysed. The product percentages after hydrolysis of maltoligosaccharides by FERMENTA are shown in Table 3. The major products obtained depended on the substrat used: maltotriose was produced from maltoheptaose and maltohexaose; maltose from maltopentaose; glucose from maltotetraose. To reach these results, two bonds have to be cut in maltotetraose and maltopentaose, while two, three or four cuts were necessary in maltohexaose and maltoheptaose.

4. Discussion

From the purified enzyme from *L. fermentum*, we studied the interaction of α-amylase with its substrate and the mode of action of FERMENTA using long and short substrates. The method is based on determination of the cleavage frequencies and on the catalytic efficiency rates. The functional study was carried out with initial substrate concentrations that were sufficiently weak to avoid bimolecular reactions such as condensation and transglycosylation.

4.1. Maltoheptaose and maltohexaose hydrolysis

Products hydrolysed at various substrate concentrations were analyzed by HPAEC (Fig. 2). Product distributions varied according to the initial substrate concentrations. In the case of maltoheptaose hydrolysis, the profile obtained at 500 μM differed from that obtained at 750 and 1000 μM. The difference may dependent on the α-amylase conformation at different concentration and the accessibility of its active and of binding sites. The maltoheptaose profiles showed the presence of glucose (about 10%) and the absence of maltopentaose. This is closer to the porcine pancreatic α-amylase profile than to the barley α-amylase profile. By contrast, maltohexaose hydrolysis gave similar profiles, regardless of the concentration. In this case, the hydrolysis profile was close to that of PPA [20].

The FERMENTA hydrolysis pattern indicated an endo-amylase, producing maltotriose, maltose and maltotetraose, and no specific cleavage was observed on oligosaccharides. This pattern was in agreement with many other α-amylases studied previously.

4.2. Catalytic efficiencies

This α-amylase showed Michaelis–Menten kinetics for maltooligosaccharides and amylose hydrolysis. The k_{cat}/K_m value increased with the chain length from maltose ($8.7 \times 10^4\ M^{-1}\ s^{-1}$) to maltoheptaose ($1.9 \times 10^7\ M^{-1}\ s^{-1}$), and then to amylose ($1 \times 10^9\ M^{-1}\ s^{-1}$). With amylose as substrate, the results showed that this amylase has one active site and binds to only one substrate molecule. The catalytic efficiency rate of FERMENTA was within the same order of magnitude as that of AMY ($1 \times 10^9\ M^{-1}\ s^{-1}$) [14] and 20-fold less active than PPA and an α-amylase from *L. plantarum* (12.6×10^9 and $20 \times 10^9\ M^{-1}\ s^{-1}$) [4,25].

Full analysis of the FERMENTA digestion products enabled us to determine the catalytic efficiencies of various maltooligosaccharides. A 10^4-fold increase in catalytic efficiency was observed from maltose to amylose. The increase in catalytic efficiency was due to the increase in the energy of the substrate-enzyme interaction and to the increase in the probability of formation of productive complexes. All FERMENTA catalytic efficiencies obtained with the maltooligosaccharide series were higher than those of PPAI and PPAII [15].

4.3. FERMENTA action pattern

The action pattern of FERMENTA was examined using the maltooligosaccharide series (G2–G7) to determine the glycosidic linkage being cleaved as well as the cleavage frequency tested by high performance liquid chromatography (HPAE-PAD). The concentration of glycosidic fragments produced by the α-amylase reaction showed linearity over the reaction time course and the product distributions were calculated for a given substrate (insert Fig. 5). The action pattern is a description of the way an enzyme attacks its substrate from the standpoint of the point of attack on the substrate and the product formation sequence (Fig. 6). In a very slow reaction, G3 is cleaved to maltose and glucose. It was found that three maltooligosaccharides substrates (G5, G6, and G7) have more than one bond cleaved, i.e. four cleavages occur in G7, three and two were hydrolysed in G6 and G5, repectively. FERMENTA readily cleaved the third linkage from the reducing end of maltooligosaccharides, the second was easy but the first was highly resistant.

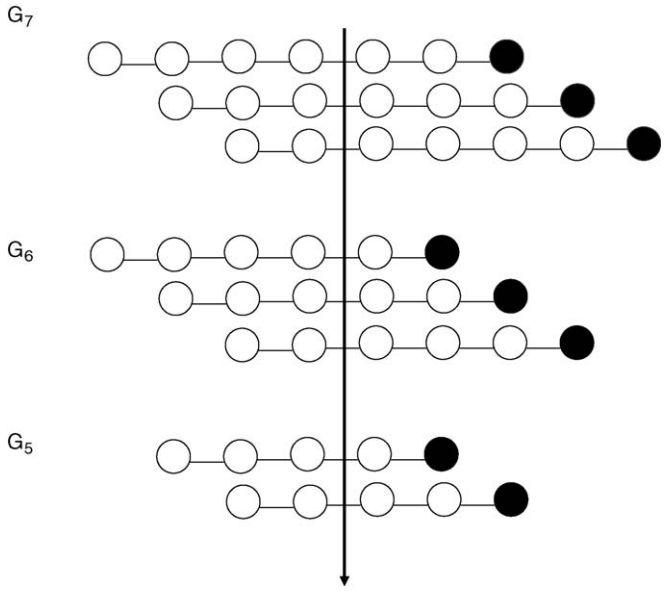

Fig. 6. Schematic representation of the main bond cleavage frequencies of FERMENTA with G5, G6, and G7: (◯) glycosyl residues; (●) reducing end; (—) linkages; and (↓) catalytic site.

The substrate specificity of FERMENTA was determined against maltooligosaccharides and polysaccharides. Use of an oligosaccharide series was helpful for determining the preferred points of attack. The terminal linkages in oligosaccharides were resistant to attack, expecially at the reducing end. FERMENTA may therefore preferentially cleave at the α-1,4 linkage adjacent to non-reducing ends, releasing maltotriose and maltose. This hydrolysis pattern of this α-amylase was consistent with an endo-type amylase. The action pattern is an initial mechanistic description mainly concerning compounds that could potentially be isolated, and they could be further studied by X-ray structural analysis in order to gain insight into the hydrolysis mechanisms. Moreover, reducing end labeled substrates could also bring complementary information on these α-amylase subsites.

Acknowledgements

The authors thank Professor A. Puigserver and Professor G. Marchis-Mouren of the Institut Méditerranéen de Recherche en Nutrition for their helpful collaboration and are grateful to V. Desseaux and E.H. Ajandouz for critical reading of the manucript.

References

[1] J.K. Chavan, S.S. Kadam, Crit. Rev. Food Sci. Nutr. 28 (1989) 351.
[2] I. MacDonald, Carbohydrates, in: Shils, M.E. Young, V.R. (Eds.), Modern Nutrition in Health and Disease, 7th ed., Lea and Febiger, Philadelphia, 1988, p. 1694.
[3] V. Agati, J.P. Guyot, J. Morlon-Guyot, P. Talamond, D.J. Hounhouigan, J. Appl. Microbiol. 85 (1998) 512.
[4] P. Talamond, V. Desseaux, Y. Moreau, M. Santimone, G. Marchis-Mouren, Comp. Biochem. Physiol. Part B. 133 (2002) 351.
[5] L. Pasero, Y. Pierron, B. Abadie, Y. Chicheportiche, G. Marchis-Mouren, Biochim. Biophys. Acta 869 (1986) 147.
[6] B. Svensson, F. Mundy, R.M. Gibson, I. Svendson, Carlsberg Res. Commun. 50 (1985) 15.
[7] M. Al Kazaz, V. Desseaux, G. Marchis-Mouren, F. Payan, E. Forest, M. Santimone, Eur. J. Biochem. 241 (1996) 787.
[8] N. Oudjeriouat, Y. Moreau, M. Santimone, B. Svensson, G. Marchis-Mouren, V. Desseaux, Eur. J. Biochem. 270 (2003) 3871.
[9] G.J. Davies, B. Henrissat, Structure 3 (1995) 853.
[10] P.T. Nix, R.D. Goldfarb, S. Morgenstern, L.J. Strong, R.C. Trivedi, Clin. Chem. 24 (1978) 1000.
[11] J.J. Marshall, A.P. Iodice, W.J. Whelan, Clin. Chim. Acta 76 (1977) 277.
[12] E.O. Haegele, E. Schaich, E. Rauscher, P. Lehmann, N. Grassl, J. Chromatogr. 233 (1981) 69.
[13] A.W. MacGregor, J.E. Morgan, E.A. MacGregor, Carbohydr. Res. 227 (1992) 301.
[14] E. Prodanov, C. Seigner, G. Marchis-Mouren, Biochem. Biophys. Res. Commun. 122 (1984) 75.
[15] C. Seigner, E. Prodanov, G. Marchis-Mouren, Biochim. Biophys. Acta 913 (1987) 200.
[16] E.H. Ajandouz, J. Abe, B. Svensson, G. Marchis-Mouren, Biochim. Biophys. Acta 1159 (1992) 193.
[17] J.A. Thoma, G.V.K. Rao, C. Brothers, J. Spradlin, J. Biol. Chem. 246 (1971) 5621.
[18] T. Suganuma, R. Masuno, M. Ohnishi, K. Hiromi, J. Biochem. 84 (1978) 293.
[19] K. Hiromi, M. Ohnishi, A. Tanaka, Mol. Cell. Biochem. 51 (1983) 79.
[20] E.H. Ajandouz, G. Marchis-Mouren, Carbohydr. Res. 268 (1995) 267.
[21] M. Qian, S. Spinelli, H. Driguez, F. Payan, Protein Sci. 6 (1997) 2285.
[22] C. Gilles, J.P. Astier, G. Marchis-Mouren, C. Cambillau, F. Payan, Eur. J. Biochem. 238 (1996) 561.
[23] Y. Chen, C. Fringant, M. Rinaudo, Carbohydr. Polym. 33 (1997) 73.
[24] S. Dygert, L.H. Li, D. Florida, J.A. Thoma, Anal. Biochem. 13 (1965) 367.
[25] R. Koukiekolo, V. Berre-Anton, V. Desseaux, Y. Moreau, P. Rouge, G. Marchis-Mouren, M. Santimone, Eur. J. Biochem. 265 (1999) 20.